Supplemental Materials

February 9, 2023

This document provides supplemental materials for the manuscript entitled "Sectorial Coverage Control with Load Balancing in Non-Convex Hollow Environments", and it is composed of two parts. The first part presents the application of proposed sectorial coverage algorithm to facility, and the second part provides the simulation results on a non-convex hollow environment. It is worth pointing out that the citation/ID numbers of equations and formulas in this supplemental material are consistent with those in the aforementioned manuscript.

1 Application to facility location

The theoretical results in the manuscript can be employed to solve the classic location optimization problem [Cortes *et al.*, 2004], where the function $f(q_i, p) = \|p_i - q\|^2$ quantifies the cost of the i-th agent to service the event occurred at the point q. According to (3), this allows us to get the following performance index

$$J(\varphi, \mathbf{p}) = \sum_{i=1}^{N} \int_{E_i(\varphi)} \|p_i - q\|^2 \rho(q) dq.$$

For the above facility location problem, we obtain two corollaries as follows.

Corollary 1.1. *For MAS (4), the control law (6) drives each agent to arrive at the centroid of subregion, i.e.* $\lim_{t\to\infty} p_i(t) = c^*_{E_i}$, $\forall i \in \mathbb{I}_N$.

Proof. It follows from $f(p_i, q) = \|p_i - q\|^2$ and the cost function (3) that

$$\begin{aligned}
\nabla_{p_i} J &= 2\int_{E_i} \rho(q)(p_i - q)^T dq \\
&= 2p_i \int_{E_i} \rho(q) dq - 2\int_{E_i} q\rho(q) dq \\
&= 2m_i(p_i - c_{E_i}), \quad \forall i \in \mathbb{I}_N,
\end{aligned}$$

where

$$c_{E_i} = \frac{\int_{E_i} q\rho(q)\,dq}{\int_{E_i} \rho(q)dq}$$

represents the centroid of subregion E_i. According to Claim 2) in Theorem 3.1, one has $\lim_{t\to\infty} \|\nabla_{p_i} J\| = 0$. Considering that $\|\nabla_{p_i} J\| = 2m_i\|p_i - c_{E_i}\|$ and $\lim_{t\to\infty} m_i(t) = \overline{m} > 0$ according to Lemma 3.1, it follows that

$$\begin{aligned}\lim_{t\to\infty} \|\nabla_{p_i} J\| &= 2\lim_{t\to\infty} m_i(t) \cdot \lim_{t\to\infty} \|p_i - c_{E_i}\| \\ &= 2\overline{m} \cdot \lim_{t\to\infty} \|p_i - c_{E_i}\| = 0,\end{aligned}$$

which leads to $\lim_{t\to\infty} \|p_i(t) - c_{E_i}(t)\| = 0$. Moreover, note that $c_{E_i} = (c_{E_i}^x, c_{E_i}^y)$ is a continuous function of φ_i, $i \in \mathbb{I}_N$, and it can be computed as

$$c_{E_i}^x = \frac{1}{m_i}\int_{\varphi_i}^{\varphi_{i+1}} \omega_x(\theta)d\theta, \quad c_{E_i}^y = \frac{1}{m_i}\int_{\varphi_i}^{\varphi_{i+1}} \omega_y(\theta)d\theta$$

with $\omega_x(\theta) = \int_{r_{in}(\theta)}^{r_{out}(\theta)} r\cos(\theta)\rho(r,\theta)\,rdr$ and $\omega_y(\theta) = \int_{r_{in}(\theta)}^{r_{out}(\theta)} r\sin(\theta)\rho(r,\theta)\,rdr$. According to Lemma 3.5, one has

$$\lim_{t\to\infty} c_{E_i}(t) = \lim_{\varphi_i \to \varphi_i^*} c_{E_i}(\varphi_i) = c_{E_i}^*, \quad i \in \mathbb{I}_N.$$

Since $0 \le \|p_i(t) - c_{E_i}^*\| = \|p_i(t) - c_{E_i}(t) + c_{E_i}(t) - c_{E_i}^*\| \le \|p_i(t) - c_{E_i}(t)\| + \|c_{E_i}(t) - c_{E_i}^*\|$, it allows us to obtain

$$\begin{aligned}0 &\le \lim_{t\to\infty} \|p_i(t) - c_{E_i}^*\| \\ &\le \lim_{t\to\infty} \|p_i(t) - c_{E_i}(t)\| + \lim_{t\to\infty} \|c_{E_i}(t) - c_{E_i}^*\| = 0,\end{aligned}$$

which implies $\lim_{t\to\infty} p_i(t) = c_{E_i}^*$. The proof is thus completed. □

Corollary 1.1 allows to optimize the coverage performance with load balancing among subregions. In comparisons, the Voronoi partition approach in [Cortes *et al.*, 2004] is not guaranteed to equalize the workload and fails to quantify the coverage performance in theory by estimating the error between the optimal coverage performance and the actual performance.

Remark 1.1. *For fixed partitions, $\varphi = (\varphi_1, \varphi_2, ..., \varphi_N)^T$ is a constant vector and the cost function (3) is the continuous function of state variables $\mathbf{p} = (p_1, p_2, ..., p_N)^T$. Then it follows from $\nabla_{p_i} J = 2m_i(p_i - c_{E_i}) = 0$, $\forall i \in \mathbb{I}_N$ that the set of centroid $\mathbf{p}^* = (c_{E_1}, c_{E_2}, ..., c_{E_N})$ is the unique critical point of the cost function (3). Moreover, its Hessian matrix is positive definite at the critical point $\mathbf{p}^*$. Thus, the cost function (3) is strictly convex with respect to state variables $\mathbf{p}$. This indicates that the set of centroid ensures the minimum of cost function (3) with fixed partitions.*

By treating $\dot{\varphi}$ as the system input and $\sqrt{m_i}(p_i - c_{E_i})$ as the system state, it is demonstrated that multi-agent system with partition dynamics is input-to-state stable.

Corollary 1.2. *MAS governed by (4) and control law (6) is input-to-state stable.*

Proof. The time derivative of (3) with respect to the compound dynamics (2) and (4) is given by

$$\begin{aligned}\frac{dJ}{dt} &= \sum_{i=1}^{N} \frac{\partial J}{\partial p_i}\dot{p}_i + \sum_{i=1}^{N} \frac{\partial J}{\partial \varphi_i}\dot{\varphi}_i \\ &= 2\sum_{i=1}^{N} m_i (p_i - c_{E_i})^T \dot{p}_i + \sum_{i=1}^{N} \dot{\varphi}_i \left[\eta(\varphi_i, p_{i-1}) - \eta(\varphi_i, p_i)\right] \\ &= -2\kappa_p \sum_{i=1}^{N} m_i \|p_i - c_{E_i}\|^2 + \sum_{i=1}^{N} \dot{\varphi}_i \left[\eta(\varphi_i, p_{i-1}) - \eta(\varphi_i, p_i)\right]\end{aligned}$$

with

$$\begin{aligned}\eta(\theta, s) = &\int_{r_{in}(\theta)}^{r_{out}(\theta)} \rho(\theta, r) r^3 dr + \|s\|^2 \cdot \int_{r_{in}(\theta)}^{r_{out}(\theta)} \rho(\theta, r) r dr \\ &- 2s^T \int_{r_{in}(\theta)}^{r_{out}(\theta)} \rho(\theta, r) \begin{pmatrix} r\cos\theta \\ r\sin\theta \end{pmatrix} r dr.\end{aligned}$$

In light of the parallel axis theorem, one has

$$J = \sum_{i=1}^{N} \int_{E_i} \rho(q) \|q - c_{E_i}\|^2 dq + \sum_{i=1}^{N} m_i \|p_i - c_{E_i}\|^2,$$

which leads to

$$\begin{aligned}\frac{dJ}{dt} &= \sum_{i=1}^{N} \frac{\partial}{\partial \varphi_i} \int_{E_i} \rho(q) \|q - c_{E_i}\|^2 dq \cdot \dot{\varphi}_i + \frac{d}{dt} \sum_{i=1}^{N} m_i \|p_i - c_{E_i}\|^2 \\ &= \sum_{i=1}^{N} \dot{\varphi}_i \left[\eta(\varphi_i, c_{E_{i-1}}) - \eta(\varphi_i, c_{E_i})\right] + \frac{d}{dt} \sum_{i=1}^{N} m_i \|p_i - c_{E_i}\|^2.\end{aligned}$$

Therefore, one gets

$$\begin{aligned}\frac{d}{dt} \sum_{i=1}^{N} m_i \|p_i - c_{E_i}\|^2 = &-2\kappa_p \sum_{i=1}^{N} m_i \|p_i - c_{E_i}\|^2 \\ &+ \sum_{i=1}^{N} \dot{\varphi}_i \left[\eta(\varphi_i, p_{i-1}) - \eta(\varphi_i, p_i)\right] \\ &- \sum_{i=1}^{N} \dot{\varphi}_i \left[\eta(\varphi_i, c_{E_{i-1}}) - \eta(\varphi_i, c_{E_i})\right].\end{aligned}$$

Let $H(t)=\sum_{i=1}^{N} m_i\|p_i-c_{E_i}\|^2$ and $e_\eta(\varphi_i,p_i,p_{i-1})=\eta(\varphi_i,p_{i-1})-\eta(\varphi_i,p_i)-\eta(\varphi_i,c_{E_{i-1}})+\eta(\varphi_i,c_{E_i})$. Then it follows that

$$\begin{aligned}\dot{H}(t) &= -2\kappa_p H(t)+\sum_{i=1}^{N}\dot{\varphi}_i\cdot e_\eta(\varphi_i,p_i,p_{i-1})\\ &\le -2\kappa_p H(t)+\|\dot{\varphi}\|\cdot\|\mathbf{e}_\eta(\varphi,p)\|\\ &\le -2\kappa_p H(t)+\|\dot{\varphi}(t)\|\cdot\sup_{\varphi\in[0,2\pi],p\in\Omega}\|\mathbf{e}_\eta(\varphi,p)\|\end{aligned}$$

with $\dot{\varphi}=(\dot{\varphi}_1,\dot{\varphi}_2,...,\dot{\varphi}_N)^T$ and

$$\mathbf{e}_\eta(\varphi,p)=(e_\eta(\varphi_1,p_1,p_N),...,e_\eta(\varphi_N,p_N,p_{N-1}))^T.$$

Solving the above differential inequality yields

$$\begin{aligned}H(t) &\le H(t_0)e^{-2\kappa_p(t-t_0)}\\ &\quad+\sup_{\varphi\in[0,2\pi],p\in\Omega}\|\mathbf{e}_\eta(\varphi,p)\|\cdot\int_{t_0}^{t}e^{2\kappa_p(\tau-t)}\|\dot{\varphi}(\tau)\|d\tau\\ &\le H(t_0)e^{-2\kappa_p(t-t_0)}\\ &\quad+\sup_{\varphi\in[0,2\pi],p\in\Omega}\|\mathbf{e}_\eta(\varphi,p)\|\cdot\frac{\sup_{\tau\in[t_0,t]}\|\dot{\varphi}(\tau)\|}{2\kappa_p},\end{aligned}$$

which implies input-to-state stability of MAS (4) driven by (6) according to the definition [Khalil, 1996].

□

2 Numerical simulations

The classic location optimization problem is taken into account by adopting the function $f(p_i,q)=\|p_i-q\|^2$. The proposed approach consists of partition procedure and subregion coverage. Specifically, the first part allows to partition the region into subregions with equal workload, while the second one enables agents to arrive at the centroid of subregions. As described in Table 1 (i.e., Algorithm 1 in the manuscript), the i-th agent moves towards its centroid $\mathbf{c}_{E_i}$ while attempting to balance workload among subregions. Here, the proposed coverage control algorithm is implemented using MATLAB R2018b, and simulation results are illustrated in Fig. 1 with 4 snapshots displaying the simulation process of 8 mobile agents. In Fig. 1, blue circles denote the mobile agents, and blue lines refer to the common boundary between agents. In addition, green stars refer to the subregion centroids. The coverage region Ω is annular area embedded with a hole, and the polar equations of inner and outer boundaries are given

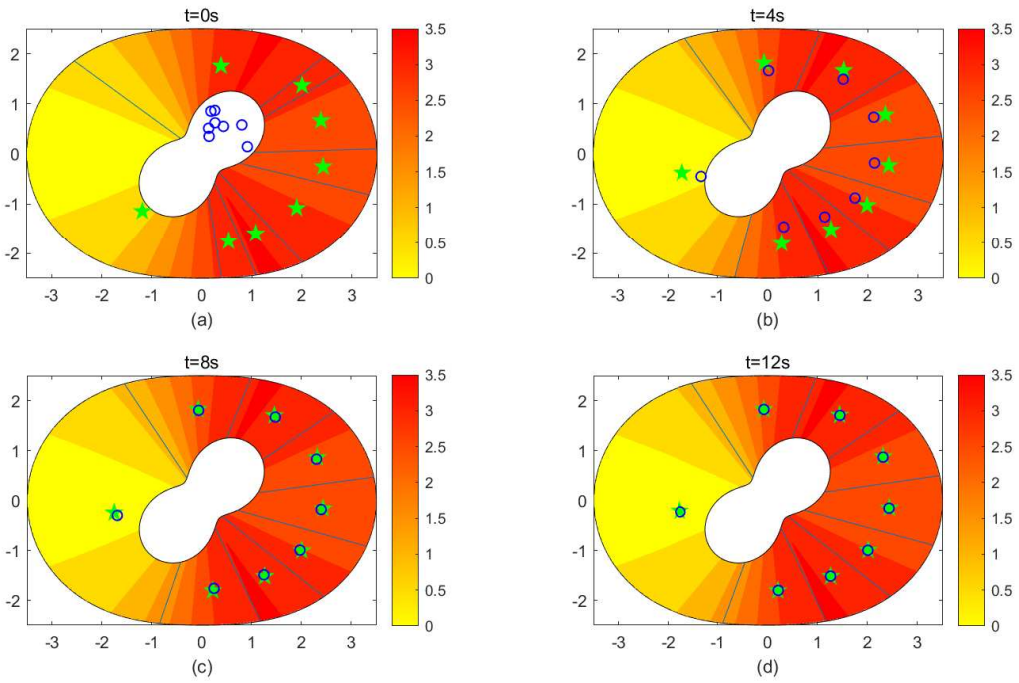

Figure 1: Snapshots of the simulation results on region partition, subregion centroids and positions in MASs. Blue circles denote the mobile agents, and green stars refer to the subregion centroids.

as $r_{in}(\theta) = 1 + 0.5\sin 2\theta$ and $r_{out}(\theta) = 3 + 0.5\cos 2\theta$, respectively. Moreover, the workload density is characterized by $\rho(r,\theta) = e^{(\sin^2\theta + \cos\theta)} + 0.01r$. Other parameters are empirically picked as follows: $\kappa_p = 0.1$, $\kappa_\varphi = 0.03$, $K^* = 30$.

In the simulation, MASs and phase angles of partition bars are initialized at random. At the time $t = 4$s, the workload partition is under way and all agents are moving towards the centroid of their respective subregions. At the time $t = 8$s, these agents get close to the centroid of subregion further, and workload equalization is almost completed. Note that the subregion centroid evolves with partition bars. At the time $t = 12$s, each agent arrives at its own centroid of subregion and partition bars converge to the desired configuration. As observed in Fig. 1, each agent eventually arrives at the centroid of its own subregion in spite of the hole in the coverage region. Figure 2 presents time evolution of state variables on the coverage control algorithm. The first variable is related to the control strength for multi-agent deployment (i.e., $\|u_i\|$), which converges to zero as time goes on. The second one describes the workload on each subregion, and they converge to the same value in the end. The last one represents the phase angle of partition bar, and these phase angles converge to the different values. The value of cost function decreases to 33.34 after running the circular search algorithm (i.e., Algorithm 1 in the

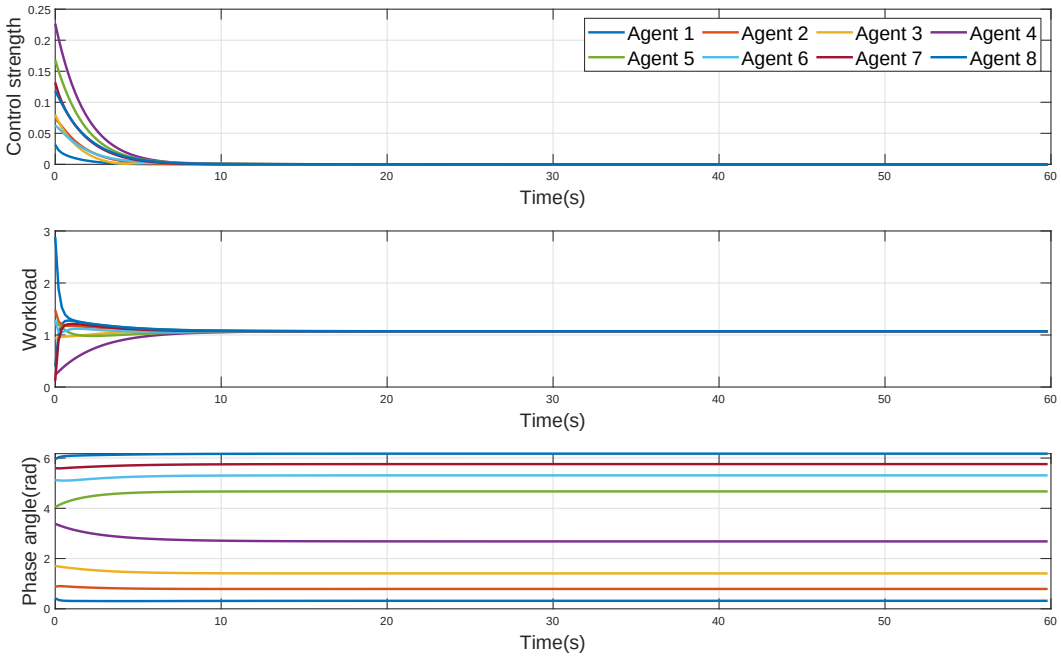

Figure 2: Time evolution of the state variables during MAS coverage.

manuscript). It is verified that the proposed algorithm is feasible in the optimization of service cost and workload equalization.

References

[Cortes *et al.*, 2004] J. Cortes, S. Martinez, T. Karatas, and F. Bullo (2004). Coverage control for mobile sensing networks. *IEEE Transactions on Robotics and Automation* 20(2), 243-255.

[Khalil, 1996] H. Khalil (1996). Nonlinear Systems, Prentice-Hall, New Jersey.